ORIGINAL RESEARCH

Silencing of LINC01116 suppresses the development of oral squamous cell carcinoma by up-regulating microRNA-136 to inhibit FN1

Zhifeng Chen[1]
Qian Tao[2,3]
Bin Qiao[4]
Leitao Zhang[1]

[1]Department of Oral and Maxillofacial Surgery, Nanfang Hospital, Southern Medical University, Guangzhou 510515, People's Republic of China; [2]Department of Oral and Maxillofacial Surgery, Guanghua School and Hospital of Stomatology, Sun Yat-sen University, Guangzhou 510055, People's Republic of China; [3]Guangdong Provincial Key Laboratory of Oral Diseases, Sun Yat-sen University, Guangzhou 510055, People's Republic of China; [4]Department of Oral and Maxillofacial Surgery, The First Affiliated Hospital of Zhengzhou University, Zhengzhou 450052, People's Republic of China

Background: Oral squamous cell carcinoma (OSCC), one of the most common cancers worldwide with a high mortality rate, is accompanied by poor prognosis, highlighting the significance of early diagnosis and effective treatment. Long non-coding RNAs (lncRNAs) have been linked with the development and progression of various cancers. In this study, aberrantly expressed lncRNA LINC01116, microRNA-136 (miR-136), and fibronectin1 (FN1) were identified in OSCC using a microarray analysis. Therefore, this study aimed to investigate the role of LINC01116/miR-136/FN1 regulatory axis in OSCC.

Methods: The gain-of-function and loss-of-function experiments in vitro were performed to alter the expression of LINC01116 and miR-136 in OSCC cells to elucidate their effects on cellular processes, including epithelial–mesenchymal transition (EMT), viability, invasion, and migration. In addition, the interaction among LINC01116, miR-136, and FN1 was identified. Additionally, the tumorigenicity and lymph node metastasis (LNM) affected by LINC01116 were observed through xenograft tumor in nude mice.

Results: LINC01116 and FN1 were abundant in both OSCC tissues and cells, while miR-136 was poorly expressed. LINC01116 could competitively bind to miR-136, which targets and negatively regulates FN1. Moreover, in response to LINC01116 silencing or miR-136 over-expression, OSCC cells exhibited diminished EMT process and inhibited cell viability, invasion, and migration in vitro, coupling with impaired tumorigenicity and LNM in vivo.

Conclusion: The fundamental findings in this study collectively demonstrate that LINC01116 silencing may inhibit the progression of OSCC *via* the miR-136-mediated FN1 inhibition, highlighting a promising therapeutic strategy for OSCC treatment.

Keywords: long non-coding RNA LINC01116, fibronectin 1, microRNA-136, oral squamous cell carcinoma, epithelial–mesenchymal transition, lymph node metastasis

Correspondence: Leitao Zhang
Department of Oral and Maxillofacial Surgery, Nanfang Hospital, Southern Medical University, No. 1838, North Guangzhou Avenue, Guangzhou, Guangdong Province 510515, People's Republic of China
Email homer120@smu.edu.cn

Bin Qiao
Department of Oral and Maxillofacial Surgery, The First Affiliated Hospital of Zhengzhou University, No. 1, Jianshe East Road, Zhengzhou, Henan Province 450052, People's Republic of China
Tel +86 0371 6686 2251
Email qiaobin@zzu.edu.cn

Introduction

Oral squamous cell carcinoma (OSCC), the 6th most prevalent cancer across the world, accounts for a majority of head and neck cancers.[1] Unfortunately, OSCC ranks the highest in relation to cancer mortality rate in comparison with the other carcinomas.[2] The etiology of OSCC involves both intrinsic factors of smoking, excessive use of alcohol, as well as betel quid chewing and extrinsic risk factor of human papillomavirus infection.[3–5] Despite improvements in cancer treatment, the overall 5-year survival rates (less than 50%) have not significantly improved over the last few decades.[6,7] The early-stage of OSCC manifests a cure rate of more than 80%, however, cannot be cured in over 70% of the patients in the advanced-stage of

OSCC.[8,9] It is widely accepted that OSCC possesses a high potential for local invasion and lymph node metastasis (LNM), LNM playing a vital role in predicting the survival of patients with OSCC, while the underlying molecular mechanism still remains to be unclear.[10] Consequently, it is urgent to investigate the early-stage detection and the detailed molecular mechanism of OSCC.

Long non-coding RNAs (lncRNAs) are a critical group of general genes that are essential to various biological functions.[11] Nowadays, several studies have demonstrated the involvement of lncRNAs in the development and progression of multiple types of cancers, including prostate, bladder, and kidney cancers.[12–15] Over-expression in lncRNA LINC01116 (LINC01116) was discovered in prostate cancer by a previous study, which concluded that the knockdown of LINC01116 with small interfering RNA (siRNA) suppressed cell proliferation in prostate cancer.[16] Another study suggested that the down-regulation of LINC01116 could inhibit cell proliferation, migration, and invasion, but contribute to apoptosis in non-small-cell lung cancer through inhibition of the Hippo signaling pathway by targeting FAT4.[17] Furthermore, lncRNAs function as read-outs of active cellular programs or signals of specific cellular states, which enables lncRNAs to identify cellular pathologies, including cancer, to be of great prognostic significance, or supplying a formula of treatment for patients suffering from cancerous diseases.[18,19] However, the role of LINC01116 in the progression of OSCC remains under-investigated.

Fibronectin 1 (FN1), belonging to the glycoprotein family of extracellular matrix, was found in a variety of cell types and associated with cellular adhesion and migration processes.[20] FN1 was also highlighted to be a potential biomarker in OSCC regarding tongue/mouth floor and edentulous ridge.[21] Besides, microRNA-1271 (miR-1271) was previously revealed to exert tumor suppressive effect on OSCC and possibly function as a promising therapeutic factor for OSCC treatment.[22] A previous study also indicated that miR-338 might serve as a potential diagnostic marker and therapeutic target for the treatment of OSCC.[23] Additionally, there is a general acceptance that miR-136 functions as a tumor suppressor gene in numerous cancers,[24,25] yet its involvement in OSCC is not fully understood. Therefore, the mechanism was identified and characterized by which LINC01116 and its target miR-136 regulated cell adhesion and migration regulator FN1. The tumor suppressor

function of miR-136 was represented, as well as the elevated expression of which inhibits cell proliferation, invasion, migration, and reverses epithelial–mesenchymal transition (EMT). Additionally, tumor growth and LNM of OSCC are prevented by overexpressed miR-136 or underexpressed LINC01116 expression. It was revealed that down-regulated LINC01116 increased the expression of miR-136, which was able to inhibit the development of OSCC, as demonstrated in vitro and in vivo.

Materials and methods
Ethical statement
The current study was conducted with approval of the Ethics Committee of the First Affiliated Hospital of Zhengzhou University (2010025) and in accordance with the principles of *Helsinki's Declaration*. Signed informed consents were obtained from all participating patients and their families prior to tissue sample collection. All animal experiments were approved by the Ethics Committee of the First Affiliated Hospital of Zhengzhou University (2017x6002) and in accordance with *the Guide for the Care and Use of Laboratory animals* published by the US National Institutes of Health.

Microarray analysis
The expression profile data related to OSCC were screened using the Gene Expression Omnibus (GEO) database (http://www.ncbi.nlm.nih.gov/geo) with "OSCC" serving as the key word. Each expression profile data were treated with background correction and normalization by applying the Affy installation package of the R software.[26] Subsequently, the linear model-empirical Bayesian statistical method combined with the moderated *t*-test was employed to conduct nonspecific screening for expression profile data for the selection of differentially expressed lncRNA and miRNAs.[27] The miRNAs that bound to the target gene were detected using the microRNA.org website (http://34.236.212.39/microrna/home.do), the mirDB website (http://www.mirdb.org/index.html), and the mirDIP website (http://ophid.utoronto.ca/mirDIP/). Finally, the miRNAs binding to lncRNA were confirmed using the RNA22 website (https://cm.jefferson.edu/rna22/).

Study subjects
A total number of 58 patients (calculated mean age: 55 years, ranging from 29 to 76 years), comprising 36 males and 22 females, who accepted surgical resection of OSCC

at the First Affiliated Hospital of Zhengzhou University from March 2010 to April 2012 were selected as the study subjects. All patients were confirmed with their focal property as squamous cell carcinoma by means of post-operative pathological examination. No patients included in the current study underwent chemoradiotherapy or immunotherapy prior to the operation. The 7th edition AJCC (American Joint Committee on Cancer) staging of OSCC was applied as reference for carrying out staging of the obtained tissues.[28] According to clinical Tumor Node Metastasis (TNM) staging, there were 12 cases in stage I, 26 cases in stage II, and 20 cases in stage III. In addition, according to the squamous cell carcinoma staging method, 24 cases were classified as highly differentiated squamous cell carcinoma, 7 cases as moderately differentiated squamous cell carcinoma, and 27 cases as poorly differentiated squamous cell carcinoma. The follow-up lasted approximately 60 months, and the Kaplan–Meier method was used for survival analysis. During the follow-up period, recurrence of tumor or death of the patient was regarded as the end. If not, the time of the final follow-up was regarded as the end point. The overall survival (OS) time was identified as the period from the date of surgery to the date of death.

Selection and culture of cells

Human oral mucosal epithelial cells (OMECs) (SCL-0682, ATCC, Manassas, VA, USA), OSCC cell line (Tca83, ATCC, Manassas, VA, USA) were cultured in 5% fetal calf serum (FCS) Roswell Park Memorial Institute (RPMI) 1,640 medium (31800022, Gibco, Grand Island, NY, USA), while TSCCa, NB, and NT were cultured in Dulbecco's Modified Eagle Medium (DMEM) containing 10% FCS. Tca8113 was cultured in an incubator in F12K medium (21127022, Gibco, Grand Island, NY, USA) in an incubator (thromo3111, Shandong Biobase Chemical Co., Ltd., Jinan, Shandong, China) with 5% CO2 in air at 37°C. Reverse transcription quantitative polymerase chain reaction (RT-qPCR) was performed to determine the expression of LINC01116 to select cell lines for subsequent experimentation.

Cell treatment

Cell transfection was conducted using Lipofectamine Transfection Reagent 2000 (11668019, Invitrogen Life Technology Co., Ltd., Carlsbad, CA, USA). After 6 hrs of transfection, the cells were further cultured in complete medium at 37°C for 48 hrs and then harvested.

Next, the cells were divided into the following 6 groups: the blank group (cells without any transfection), the NC group (cells transfected with empty plasmids), the siRNA-LINC01116 group (cells transfected with siRNA-LINC01116 plasmids), the miR-136 mimic group (cells transfected with miR-136 mimics), the miR-136 inhibitor group (cells transfected with miR-136 inhibitors), and the siRNA-LINC01116 + miR-136 inhibitor group (cells co-transfected with siRNA-LINC01116 and miR-136 inhibitors).

Dual luciferase reporter gene assay

The RNA22 software website was employed to predict the binding sites of miR-136 with LINC01116 and FN1. The target fragments were cloned into the downstream region of the luciferase reporter pmirGLO (3577193, Promega Biotech Co., Ltd., Madison, WI, USA) using double enzyme digestion, and then named LINC01116-wild type (wt) and FN1-wt. Site-directed mutagenesis of the binding sites was performed to construct the LINC01116-mutant (mut) and FN1-mut vectors. MiR-136 mimics and miR-136 NC were co-transfected with control sequences according to the instructions of LipofectamineTM 2000 (Invitrogen Life Technology Co., Ltd., Carlsbad, CA, USA). A luminometer (GloMax® 20/20, Promega Biotech Co., Ltd., Madison, WI, USA) was used to detect cell luciferase activity in accordance with the instructions of Dual Luciferase Reporter Assay Kit (E1910, Promega Biotech Co., Ltd., Madison, WI, USA), and the luciferase activity was calculated as follows: the luciferase activity=the firefly luciferase activity/the renilla luciferase activity.

RNA pull-down assay

Cells were transfected with 50 nM biotin-labeled WT-bio-miR-136 and MUT-bio-miR-136 (Genecreat Biotech Co., Ltd., Wuhan, Hubei, China). Subsequently, the cells were collected and thoroughly rinsed using phosphate buffer saline (PBS) after 48 hrs and furthermore incubated in specific lysate buffer (Ambion, Austin, Texas, USA) for 10 mins. Subsequently, the lysates were incubated with the M-280 streptavidin beads (S3762, Sigma-Aldrich Corp. St. Louis, MO, USA) that were pre-coated with Ribonuclease (RNase)-free bovine serum albumin (BSA) and yeast tRNA (TRNABAK-RO, Sigma-Aldrich Corp. St. Louis, MO, USA) for 3 hrs at 4°C. The beads were washed twice using pre-cooled lysate buffer solution, three times with low-salt buffer solution, and once with high-salt

buffer solution. The bound RNAs were purified using Trizol while LINC01116 enrichment was detected by qPCR.

RNA binding protein co-immunoprecipitation (RIP) assay

A RIP kit (Millipore, Temecula, CA, USA) was employed to detect the binding of LINC01116 with argonaute2 (AGO2) protein. Neurons were rinsed with pre-cooled PBS, with the supernatant removed. The cells were lysed with an equal volume of RIPA lysis buffer (P0013B, Beyotime Biotechnology Inc., Shanghai, China) in an ice bath for 5 mins, and centrifuged at 14,000 rpm for 10 mins at 4°C with the supernatant collected. A total of 50 μL magnetic beads were washed, re-suspended in 100 μL RIP Wash Buffer and added with 5 μg antibody according to the experimental groups for binding. The bead-antibody complex was washed, re-suspended in 900 μL RIP Wash Buffer, and added with 100 μL cell extract for incubation at 4°C overnight. Samples were placed on magnetic holders to obtain magnetic bead-protein complexes. The RNA content in samples and input were extracted with the detachment of proteinase K for subsequent PCR detection. The antibodies used in RIP were AGO2 (dilution ratio of 1:50, ab32381, Abcam, Cambridge, MA, USA), which was mixed at room temperature for 30 mins, and IgG (dilution ratio of 1:100, ab109489, Abcam, Cambridge, MA, USA), which was used as a negative control.

RNA fluorescence in situ hybridization (RNA-FISH)

Cell culture conditions were as follows: the coverslips were placed on the bottom of a 24-well plate and cells were cultured with a density of 6×10^4 cells/well. Cell confluence was allowed to reach 60–70% prior to the experiment. Cells fixation and verification were as follows: the cells were rinsed with 1× PBS for 5 mins, fixed with 4% paraformaldehyde at room temperature for 10 mins, followed by 1× PBS rinsing three times, 5 mins each time. Next, the cells in each well were added with 1 mL of pre-cooled permeable fluid, stored at 4°C for 5 mins, and rinsed again 3 times with 1× PBS, 5 mins each time. Probe detection was as follows: the cells in each well were added with 20 μL of pre-hybridization solution, followed by a blockade of the cells for 30 mins at 37°C. After discarding the pre-hybridization solution from each well, the cells were added with an appropriate amount of hybridization solution containing probes and hybridized

overnight at 37°C avoiding exposure to light. The cells in each well were washed 3 times by applying cleaning lotion I at 42°C (5 mins each time), followed by an additional cleaning process using lotion II and cleaning lotion III under the same conditions (1× PBS rinsing was then conducted at room temperature for 5 mins). DNA staining was as follows: the cells were stained with 4′,6-diamidino-2-phenylindole (DAPI) dye for 10 mins avoiding exposure to light and rinsed three times with 1× PBS, 5 mins each time. Sealing was as follows: under dark conditions, the coverslips were fixed on cell slide using mounting medium (eg, nail polish) for fluorescent detection.

Cell Counting Kit-8 (CCK-8) assay

After 48 hrs of transfection, cells in each group were rinsed twice with PBS, detached with 0.25% trypsin and inoculated in 96-well plates at a cell density of 1×10^4 cells/well, with 3 parallels set in each well. The cells in each well were added with 10 μL CCK-8 reagent (40203ES60, Yeasen Biotechnology Co., Ltd., Shanghai, China) at 0 hr, 24 hrs, 48 hrs, and 72 hrs post culture. After 4 hrs of incubation, the optical density (OD) of each well was measured with an excitation wavelength of 450 nm using a microplate reader (MK3, Thermo Fisher Scientific, San Jose, California, USA). The cell viability curve was plotted with time point as the abscissa and the OD as the ordinate. Each experiment was repeated 3 times to obtain the mean value.

Scratch test

After 48 hrs of transfection, a marker pen was used to draw a horizontal line across the well at an interval of approximately 0.5–1 cm at the back of the 6-well plate. Approximately 5 lines were marked across each well. Nearly 5×10^5 cells were added and allowed to settle on the plate overnight. The following day, with the help of a ruler, scratches were created using a pipette tip perpendicular to the horizontal lines at the back of the plate without tilting. The cells were rinsed 3 times with PBS to remove cellular debris prior to the addition of serum-free medium. Then, the cells were placed in an incubator with 5% CO_2 in air at 37°C. Photos were collected and observed at the 0 hr and 48 hrs.

Transwell assay

After 48 hrs of transfection, the Matrigel gel (YB356234, YU BO Biological Technology Co., Ltd., Shanghai, China) stored at −80°C was collected and thawed into liquid at 4°C overnight. Moreover, 200 μL Matrigel gel (356235, Haoran

Biological Technology Co., Ltd., Shanghai, China) was diluted in 200 μL serum-free medium at 4°C. Next, 50 μL of mixture was added to the apical chambers of Transwell plate and placed in an incubator for 2–3 hrs. Afterwards, 200 μL cell suspension was added to the apical chamber of each well, while 800 μL conditioned medium containing 20% FBS was added to the basolateral chamber. Following incubation for 20–24 hrs at 37°C, the Transwell plate was removed, rinsed twice using PBS, immersed in formaldehyde for 10 mins, and washed 3 times. The cells were stained with 0.1% crystal violet at room temperature for 30 mins, rinsed twice with PBS, and the remaining cells on the upper surface were wiped off using a cotton swab. After drying, 5 fields were randomly selected with cells counted using an inverted microscope (Leica, Wetzlar, Germany) and the average was obtained. This experiment was repeated 3 times to obtain the mean value.

RT-qPCR

After 48 hrs of transfection, cells of each group were harvested for further experiments. Trizol (Biosentech Biotechnology Co., Ltd., Beijing, China) was used to extract total RNA content from the cells and tissues, with the concentration and purity determined. According to the instructions of ReverTra Ace qPCR RT Kit (FSQ-101, TOYOBO Co., Ltd., Osaka, Osaka Prefecture, Japan), the sample was placed in a PCR amplification instrument at 25°C for 10 mins, at 37°C for 60 mins, and at 98°C for 5 mins to terminate the reaction. Based on the miR-136 reverse transcription primer (5′-GTCGTATCCAGTGCGTGTCGTGG AGTCGGCAATTGCACTGGATACGACTCCATC-3′), the RNA was reverse transcribed into cDNA. The obtained cDNA was used as a template and target genes were amplified. Both forward and reverse primers of genes were

designed, synthesized by Shanghai Sangon Biotech Company (Shanghai, China) (Table 1). RT-qPCR amplification system (20 μL) included a 2.0 μL genome template, 10 μL SYBR Premix Ex Taq (DRR041S, Takara Biomedical Technology (Beijing) Co., Ltd., Beijing, China), 0.5 μL forward primers, 0.5 μL reverse primers, and 7 μL sterilized ddH$_2$O. Glyceraldehyde-3-phosphate dehydrogenase (GAPDH) was used as the internal reference for LINC01116 and target genes, while U6 served as the internal reference for miR-136. Subsequently, a Real-Time PCR System (4485694, Thermo Fisher Scientific, San Jose, California, USA) platform was applied for detection. The CT value (inflection point of amplification power curve) was calculated using the following formulas: ΔCt=CT (target gene)−CT (internal reference), ΔΔCt=ΔCt (experimental group)−ΔCt (control group) with the relative quantification method adopted and 2$^{-\Delta\Delta Ct}$ as the relative expression level of the target gene.[29] Each experiment was repeated 3 times to obtain the mean value.

Western blot analysis

Cells were harvested from each group after transfection for 48 hrs, rinsed with PBS, and re-suspended. The supernatant was obtained after centrifugation and the RIPA lysate buffer (P0013B, Beyotime Biotechnology Inc., Shanghai, China) was added at a concentration of 10^7 cells/mL, followed by the addition of an appropriate amount of phenylmethylsulfonyl fluoride (PMSF). Cells were mixed gently, re-suspended, incubated on ice, and centrifuged at 4°C for 10 mins (12,000 rpm), with the supernatant obtained, which was regarded as the total protein content of cells. The protein concentration was measured using a bicinchoninic acid (BCA) protein quantification kit (Beyotime Biotechnology Inc., Shanghai,

Table 1 The primer sequences for RT-qPCR

Gene	Forward primer (5′–3′)	Reverse primer (5′–3′)
miR-136	GGGACUCCAUUUGUUUUGAU	CAGTGCGTGTCGTGGAGT
LINC01116	TTCAAGTGCGTCCGGGTTT	CCTGCCGATTCCCCATTCC
U6	CCAGCCCATGATGGTTCTGAT	GGCTGGTAAGGATGAAGG
FN1	CGGTGGCTGTCAGTCAAAG	AAACCTCGGCTTCCTCCATAA
Vimentin	CGCCAGATGGGTGAAATGG	ACCAGAGGGAGTGAATCCACA
N-cadherin	ACAGTGGCCACCTACAAAGG	CCGAGATGGGGTTGATAATG
E-cadherin	CCCACCACGTACAAGGGTC	CTGGGGTATTGGGGGCATC
MMP-9	TGTACCGCTATGGTTACACTCG	GGCAGGGACAGTTGCTTCT
GAPDH	ACAGTCCATGCCATCACTG	AGTAGAGGCAGGGATGATG

Abbreviations: RT-qPCR, reverse transcription quantitative polymerase chain reaction; miR-136, microRNA-136; FN1, fibronectin1; E-cadherin, epithelial cadherin; N-cadherin, neural cadherin; MMP-9, matrix metalloprotein 9; GAPDH, glyceraldehyde 3-phosphate dehydrogenase.

China). Then, 20 μg of the cell total protein was separated by 10% sodium dodecyl sulfate polyacrylamide gel electrophoresis (SDS-PAGE) and then transferred onto a polyvinylidene fluoride (PVDF) membrane. The membrane was blocked for 1.5 hrs using 5% skim milk powder that was prepared using Tris-buffered saline Tween (TBST). Next, the membrane was incubated with diluted primary antibodies as follows: rabbit anti-human FN1 polyclonal antibody (ab2413, dilution ratio of 1:1,000), rabbit anti-human E-cadherin (ab40772, dilution ratio of 1:10,000), rabbit anti-human N-cadherin (ab18203, dilution ratio of 1:1,000), rabbit anti-human Vimentin (ab45939, dilution ratio of 1:1,000), rabbit anti-human matrix metalloprotein 9 (MMP-9) (ab73734, dilution ratio of 1:1,000), and rabbit anti-human GAPDH polyclonal antibody (ab9485, dilution ratio of 1:2,500). The membrane was then incubated with the corresponding secondary antibody horseradish peroxidase (HRP)-labeled goat anti-rabbit IgG (ab6721, dilution ratio of 1:10,000) at room temperature for 2 hrs. All aforementioned antibodies were purchased from Abcam (Cambridge, MA, USA). Moreover, the membrane was immersed in chemiluminescence (ECL) reaction solution (NCI4106, Shanghai Huiying Biological technology Co., Ltd., Shanghai, China) for coloration and further photographed using SmartView Pro 2000 (UVCI-2100, Major Science, Saratoga, CA, USA). The gray values of protein bands were computed using the Quantity One software.

Tumor xenografts in nude mice

A total of 30 specific pathogen-free (SPF) male BALB/c nude mice (BEIJING HFK Bioscience Co., Ltd., Beijing, China) aged 5 weeks with weight of 16–17 g were housed in an SPF-grade barrier environment at the Laboratory Animal Center, Zhengzhou University (Zhengzhou, Henan, China). All litters, cages, fodder, and drinking water for nude mice were sterilized using high temperature or ultraviolet radiation. The nude mice were maintained at 25°C with the air velocity of 20 cm^3/s and 55% relative humidity. Subsequently, the nude mice were indiscriminately divided into 6 groups, with 5 mice in each group.

Cells form each group presenting with good growth conditions state were treated with 0.25% trypsin detachment and rinsed 3 times with PBS. PBS was then used to re-suspend cells to produce a single cell suspension. Then, 100 μL cell suspension (1×10^6 cells) were inoculated subcutaneously on the back of nude mice using a No. 6 needle, and the tumor volume was measured every 3 days after subcutaneous inoculation until the 24th day. The measurement formula was as follows: tumor volume=(length×width^2)/2. The tumor growth curve was subsequently plotted accordingly.

Hematoxylin-eosin (HE) staining

The adjacent lymph nodes of tumor-bearing neoplasms of nude mice were dissected, fixed, embedded with paraffin, sliced into sections at a thickness of 4 μm, and dewaxed with xylene. The dehydration process was conducted with xylene (I) for 5 mins, toluene (II) for 5 mins, 100% ethanol for 2 mins, 95% ethanol for 1 min, 80% ethanol for 1 min, and 75% ethanol for 1 min. Subsequently, the sections were washed by distilled water for 2 mins, stained with hematoxylin for 5 mins, and rinsed thoroughly with running water. Next, the sections were dissimilated by hydrochloric acid and ethanol for 30 s (lifting and throwing for several times), immersed in running water for 15 mins or warm water (approximately 50°C) for 5 mins and stained with eosin for 2 mins. Next, gradient alcohol dehydration and clean were conducted [95% ethanol (I), 95% ethanol (II), 100% ethanol (I), 100% ethanol (II), toluene benzene carbonate (3:1), toluene (I), xylene (II), 1 min/time]. Lastly, neutral gum-mounted sections were observed and photographed under an inverted microscope (XSP-CA, Optical Instrument Factory, Shanghai, China).

Statistical analysis

All collective data were analyzed using the SPSS 21.0 statistical software (IBM Corp, Armonk, NY, USA). Measurement data were expressed as mean±standard deviation. The Student t-test was used to compare data between two groups. One-way analysis of variance (ANOVA) was employed for comparisons among multiple groups. Enumeration data were represented by the number of cases, and the difference analysis was performed using the chi-square test. The data normality test was conducted using the Kolmogorov–Smirnov method and the data with normal distribution among multiple groups were compared by applying the one-way ANOVA, with Tukey's post hoc test conducted. The data with skewed distribution were tested using the nonparametric test of Kruskal–Wallis. Values at different time points were compared using repeated measures ANOVA. A value of $p<0.05$ was considered to be statistically significant.

Results

High expression of LINC01116 and FN1 correlates with poor prognosis of patients with OSCC

According to the differential analysis of the expression profile data GSE30784, the results displayed that LINC01116 and FN1 were highly expressed in OSCC (Figure 1A). In addition, heat map analysis of the expression profile data GSE74530 and GSE37991 further confirmed the presence of high expression of LINC01116 and FN1 in OSCC (Figure 1B and C). Besides, hsa-miR-144-3p, hsa-miR-1271-5p, hsa-miR-429, hsa-miR-27b-3p hsa-miR-200c-3p, hsa-miR-96-

5p, hsa-miR-200b-3p, hsa-miR-217, hsa-miR-613, hsa-miR-206, hsa-miR-27a-3p, and hsa-miR-136-5p were potential miRNAs targeted by FN1, by means of the microRNA.org website, the miRDB website, and the mirDIP website (Figure 1D). Finally, the RNA22 website was used to determine that only LINC01116 could possibly bind to miR-136 and regulate the expression of FN1. After RT-qPCR detection on 58 cases (OSCC tissues and adjacent tissues), it was found that the expression of LINC01116 and FN1 was noticeably increased while that of miR-136 significantly decreased in OSCC tissues compared with the adjacent tissues (Figure 1E–G) (all *p*<0.05). The correlation analysis revealed a positive correlation between both the expression of
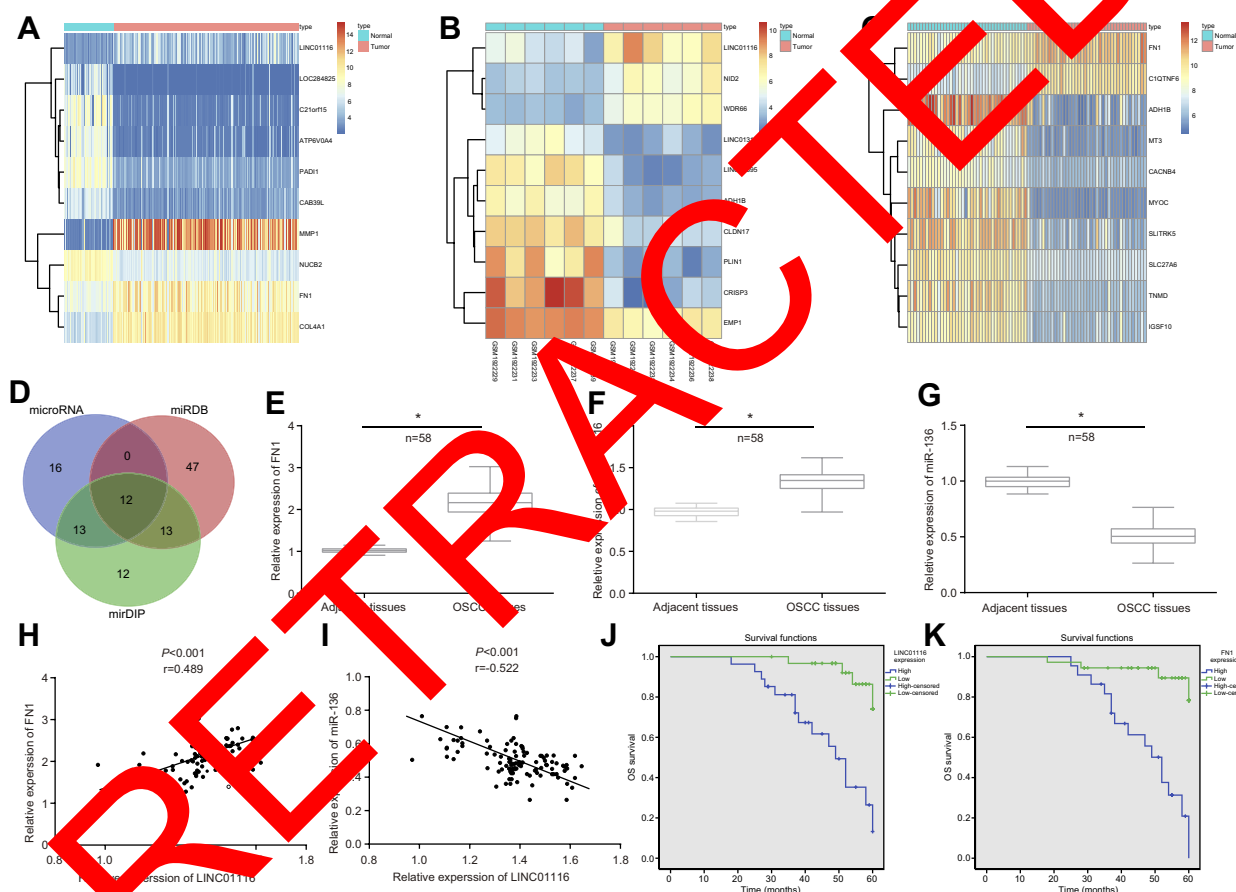
Figure 1 LINC01116 and FN1 are highly expressed while miR-136 is repressed in OSCC and related to poor prognosis. (**A**) The heat map of the microarray data GSE30784. (**B**) The heat map of the microarray data GSE74530. (**C**) The heat map of the microarray data GSE37991. The abscissa referred to the sample number, and the ordinate referred to names of differentially expressed genes. The upper right histogram represented the color gradation, the color changing from top to bottom indicated the expression value in the microarray data from high to low, each rectangle corresponded to the expression of one sample, each column showed the expression of all genes in each sample, and the left dendrogram revealed the cluster analysis results of the different genes in different samples, the uppermost bar indicated the sample type, and the upper right block indicated the sample color reference. (**D**) The microRNA.org website, miRDB website, and mirDIP website were used to predict the intersection of the miRNA of FN1. (**E**) RT-qPCR was used to determine the expression of LINC01116 in 58 cases of OSCC tissues and adjacent tissues (*p<0.05 vs adjacent tissues). (**F**) RT-qPCR was used to determine the expression of FN1 in 58 cases of OSCC tissues and adjacent tissues (*p<0.05 vs adjacent tissues). (**G**) RT-qPCR was used to determine the expression of miR-136 in 58 cases of OSCC tissues and adjacent tissues (*p<0.05 vs adjacent tissues). (**H**) The correlation analysis between the expression of LINC01116 and FN1 in OSCC tissues demonstrated a positive correlation. (**I**) The correlation analysis between the expression of LINC01116 and miR-136 in OSCC tissues demonstrated a negative correlation. (**J**) The survival analysis related to LINC01116 expression in patients with OSCC indicated that higher expression of LINC01116 was associated with poor prognosis. (**K**) The survival analysis related to FN1 expression in patients with OSCC indicated that higher expression of FN1 was associated with poor prognosis. n=58; the data were measurement data and expressed as mean±standard deviation. The *t*-test was used for comparison between two groups. *p<0.05 vs adjacent tissues.

Abbreviations: FN1, fibronectin1; miR-136, microRNA-136; OSCC, oral squamous cell carcinoma; RT-qPCR, reverse transcription quantitative polymerase chain reaction.

LINC01116 and FN1 (Figure 1H) and a negative correlation between the expression of LINC01116 and miR-136 (Figure 1I). In order to further investigate the relationship between the expression levels of LINC01116 and FN1 with the prognosis of OSCC patients, we determined the expression of LINC01116 and FN1 in tumor and adjacent tissues. Detailed information was collected from patients with OSCC. Kaplan–Meier analysis showed a poor overall survival rate of OSCC patients with high expression of FN1 or LINC01116 ($p<0.05$) (Figure 1J and K). Based on the aforementioned findings, it could be concluded that high expression of LINC01116 and FN1 found in OSCC was closely associated with poor prognosis.

The median relative expression of LINC01116 in OSCC tissues was determined to be 1.3475, which served as a reference to divide the 58 patients into the 2 following groups: patients with highly expressed LINC01116 and patients with poorly expressed LINC01116. Based on clinical pathological data, it was noticed that high expression

level of LINC01116 was correlated with TNM staging, tumor diameter, and LNM (all $p<0.05$), but no significant correlation was identified in age, gender, degree of differentiation, and depth of invasion (all $p>0.05$) (Table 2).

TSCCa and Tca83 cell lines display highest LINC01116 expression

The selection process was performed based on the expression of LINC01116 in OSCC cell lines and human OMECs. The results are shown in Figure 2: compared with the human OMECs, OSCC cell lines (TSCCa, Tca83, NB, NT, and Tca8113) exhibited significantly increased expression of LINC01116. Ranging from highest to lowest, the order of LINC01116 expression in the OSCC cell was Tca83, TSCCa, Tca8113, NT, and NB. The LINC01116 expression between TSCCa and Tca83 was found to be not significantly different ($p>0.05$). Therefore, TSCCa and Tca83 cell lines were selected for subsequent experimentation.

Table 2 Correlation analysis of LINC01116 expression and the clinicopathological features in OSCC

Clinicopathological features	Cases (n)	LINC01116 expression		p
		High expressed (n)	Poorly expressed (n)	
Age				p=0.785
≥60 years old	21	11	11	
<60 years old	37	18	18	
Gender				p= 0.588
Male	36	17	19	
Female	22	12	10	
Tumor diameter				p=0.016
≥4 cm	23	16	7	
<4 cm	35	13	22	
Degree of differentiation				p=0.792
High + Moderate	31	15	16	
Low	27	14	13	
Depth of invasion				p=0.134
T1/T2	43	19	24	
T3/T4	15	10	5	
Lymph node metastasis				p=0.009
N0	41	16	25	
N1/N2	17	13	4	
TNM staging				p=0.006
I–II stage	38	14	24	
III stage	20	15	5	

Notes: n=58; the data were enumeration data and expressed as the number of cases; the difference analysis was performed with the chi-square test. $p<0.05$ represented statistically significant difference.
**Abbreviation:** TNM, Tumor Node Metastasis.
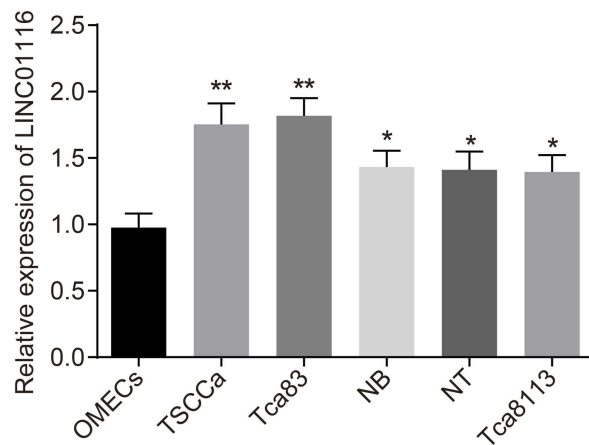
Figure 2 TSCCa and Tca83 OSCC cell lines exhibit relatively higher LINC01116 expression. The data were measurement data and expressed as mean±standard deviation. This experiment was repeated 3 times to obtain the mean value. Data between two groups were compared by independent sample *t*-test. *p<0.05 vs human OMECs, **p< 0.01.
Abbreviations: OSCC, oral squamous cell carcinoma; OMECs, oral mucosal epithelial cells.

LINC01116 can bind to miR-136 and FN1 is a target gene of miR-136

As the results of bioinformatics and dual-luciferase reporter gene assay indicated (Figure 3), the presence of a binding relationship between LINC01116 and miR-136 was evident, and miR-136 targeted FN1. In comparison to the NC group, miR-136 mimic was found to markedly inhibit the luciferase activity of LINC01116-wt (p<0.05), but did not exert the same effects on LINC01116-mut (p>0.05), suggesting that LINC01116 could competitively bind to miR-136. In comparison to the NC group, miR-136 mimic exerted no significant effect on the luciferase activity of FN1-mut 3′untranslated region (3′-UTR) (p>0.05), but weakened the luciferase activity of FN1-wt 3′-UTR (p<0.05), indicating that FN1 was the target gene of miR-136. The aforementioned data elucidated that LINC01116 could competitively bind to miR-136, which targets FN1.
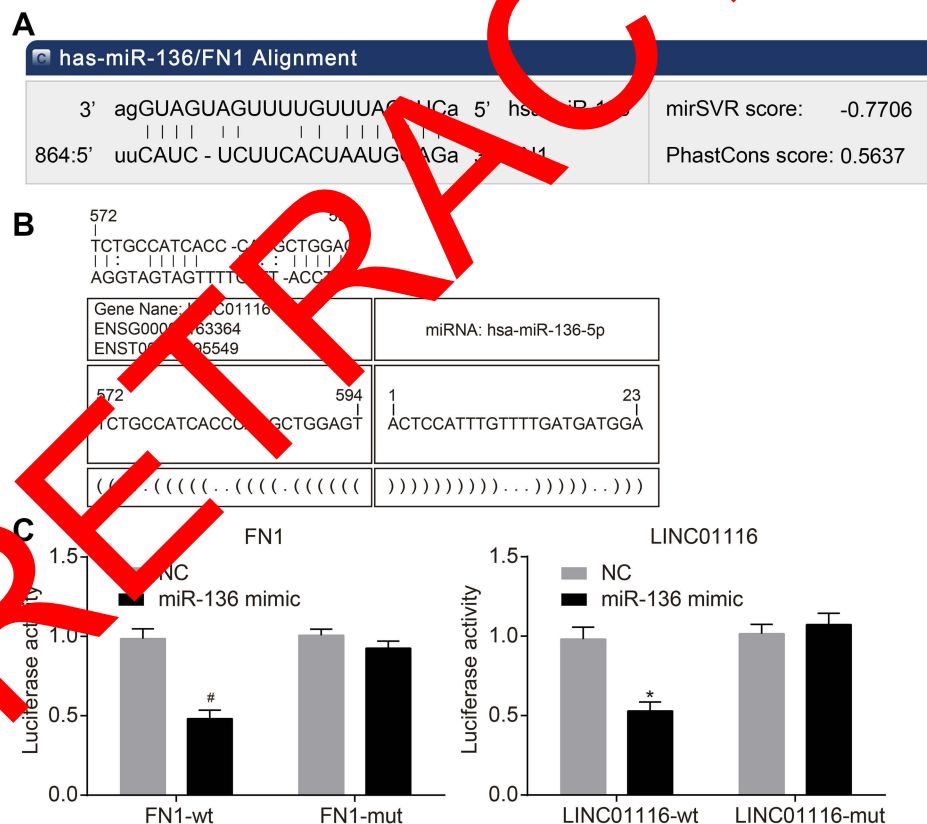
Figure 3 LINC01116 can bind to miR-136, which targets FN1. (**A**) Binding sites of miR-136 and FN1. (**B**) Binding sites of miR-136 and LINC01116. (**C**) Measurement of luciferase activity to verify the relationship of miR-136 and FN1. (**D**) Measurement of luciferase activity to verify the relationship of miR-136 and LINC01116. The data were measurement data and expressed as mean±standard deviation. This experiment was repeated 3 times to obtain the mean value. The *t*-test was used for comparison between two groups. *p<0.05 vs the LINC01116-wt + NC group; #p<0.05 vs the FN1-wt + NC group.
Abbreviations: FN1, fibronectin1; miR-136, microRNA-136; wt, wild type; NC, negative control.

LINC01116 competitively binds to miR-136

In order to further verify the interaction between LINC01116 and miR-136, RNA-pull down and RIP assay were performed. The results indicated that (Figure 4A and B): after detecting the enrichment of LINC01116 using RT-qPCR, LINC01116 enrichment in the WT-bio-miR-136 group was significantly increased in comparison to the MUT-bio-miR-136 group ($p<0.05$). In addition, anti-AGO2 antibody was found to precipitate LINC01116, indicating that LINC01116 was capable of forming a complex with AGO2. The results demonstrated that the complex of LINC01116 with AGO2 could competitively bind to miR-136 and reduce the dissociative degree of miR-136.

LINC01116 is located in the cytoplasm of OSCC cells

Subsequently, FISH assay was employed to detect the distribution of LINC01116 in OSCC cells. The results revealed (Figure 5) that LINC01116 was primarily expressed in the cytoplasm and only a minimal amount was expressed in the nucleus. The red part represented LINC01116 and the blue part represented the nucleus, indicating that LINC01116 was evidently localized to the cytoplasm.

LINC01116 silencing or miR-136 over-expression reduces cell viability of OSCC cells

Furthermore, CCK-8 assay was utilized to detect changes in cell proliferation brought about by LINC01116 and miR-136. The results showed (Figure 6) that the relative viability and proliferation rate of cells in TCCa and Tca83 cell lines were consistent. After 24 hrs, 48 hrs, and 72 hrs of cell culture, no obvious differences were detected among the OD values between the blank group and the NC group ($p>0.05$). In comparison to the blank and NC groups, the relative viability of cells in the miR-136 inhibitor group was found to be promoted significantly
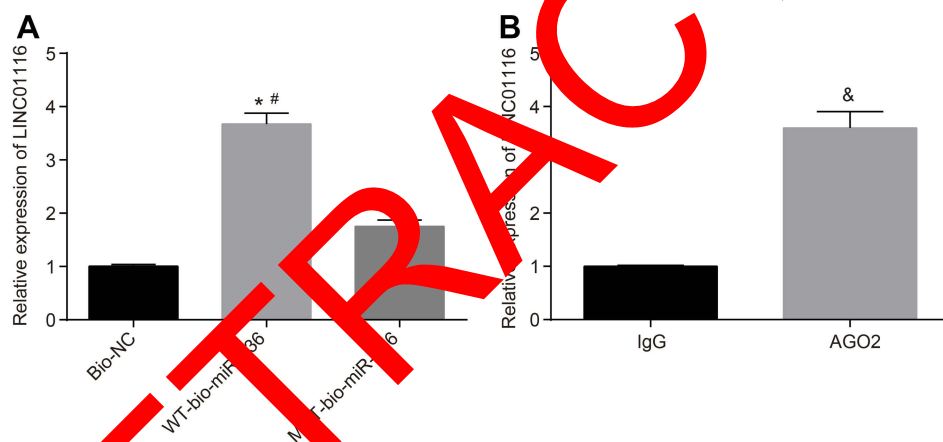
Figure 4 LINC01116 can competitively bind to miR-136. (**A**) LINC01116 can competitively bind to miR-136, verified using RNA pull-down assay. (**B**) LINC01116 can bind to AGO2 protein, verified by RIP assay. The data were the measurement data and expressed as mean±standard deviation. The experiment was repeated 3 times to obtain the mean value. The t-test was used for the comparison between two groups, while one-way ANOVA was applied for comparison among multiple groups. *$p<0.05$ vs the Bio-NC group; #$p<0.05$ vs the MUT-bio-miR-136 group; &$p<0.05$ vs IgG.
Abbreviations: miR-136, microRNA-136; AGO2, argonaute2; RIP, RNA-binding protein co-immunoprecipitation; ANOVA, analysis of variance; MUT, mutant; NC, negative control.
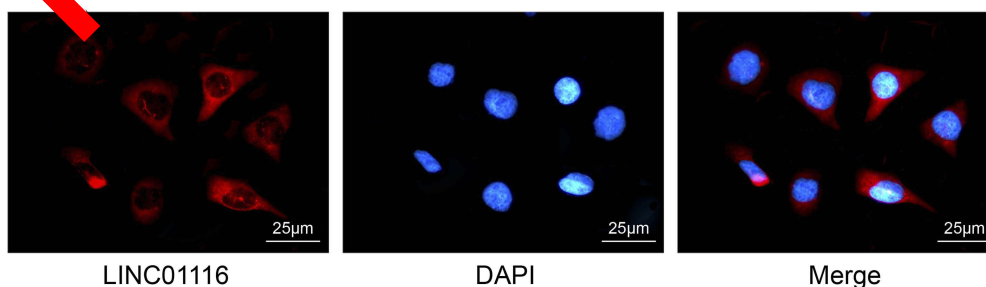
Figure 5 LINC01116 expression is located in cytoplasm of OSCC cells, as revealed by FISH assay (×400).

at 48 hrs and 72 hrs, and the proliferation of cells was accelerated (all *p*<0.05). Subsequently, the relative viability of cells in the miR-136 mimic and siRNA-LINC01116 groups was inhibited while the proliferation of cells was slowed down (all *p*<0.05). There were no significant differences in the proliferation rate of cells in siRNA-LINC 01116+ miR-136 inhibitor group when compared to the blank and NC groups (all *p*>0.05). The results indicated that LINC01116 silencing or miR-136 over-expression could inhibit the proliferation of OSCC cells.

LINC01116 silencing or miR-136 over-expression inhibits cell invasion and migration of OSCC cells

An investigation was conducted in relation to LINC01116 and miR-136 and their respective effects on invasion and migration of OSCC cells. Based on the results in Figure 7, the changing tendency of invasion and migration of the TSCCa and the Tca83 cell lines was consistent. No significant differences were found in cell migration and invasion among the blank group, the NC group, and the siRNA-LINC01116 + miR-136 inhibitor group (all *p*>0.05). In comparison to the blank and NC groups, at 48 hrs, the cell migration and invasion ability were found to be significantly inhibited in the siRNA-LINC01116 and miR-136 mimic groups, while relatively promoted in the miR-136 inhibitor group (all *p*<0.05). The results provided evidence proving that LINC01116 silencing or miR-136 over-expression could inhibit cell invasion and migration of OSCC cells.
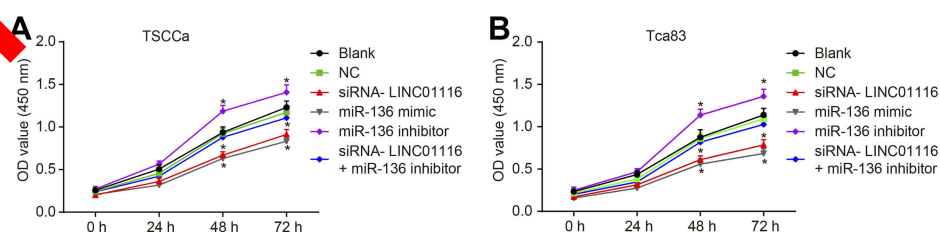
LINC01116 silencing or miR-136 over-expression inhibits EMT in OSCC cells

RT-qPCR and Western blot analysis were performed to investigate the effects of miR-136, LINC01116, and FN1 on EMT with quantified expression of EMT-related markers (E-cadherin, Vimentin, N-cadherin, and MMP-9). The

results (Figure 8) showed that the altering tendency on expression of EMT-related genes in the TSCCa cell line and the Tca83 cell line was consistent. No significant differences were found regarding the expression of EMT-related genes between the blank group and the NC group (all *p*>0.05). In comparison to the blank and NC groups, higher expression of miR-136 and E-cadherin while lower expression of LINC01116, FN1, Vimentin, N-cadherin and MMP-9 were noted in the siRNA-LINC01116 and miR-136 mimic groups (*p*<0.05). The miR-136 inhibitor group exhibited the opposite changing tendency (all *p*<0.05). However, the expression of EMT-related genes did not differ significantly in the siRNA-LINC01116 + miR-136 inhibitor group in comparison to the blank and NC groups (all *p*>0.05). The aforementioned findings suggested that silencing of LINC01116 or miR-136 over-expression could exert inhibitory effects on EMT in OSCC.
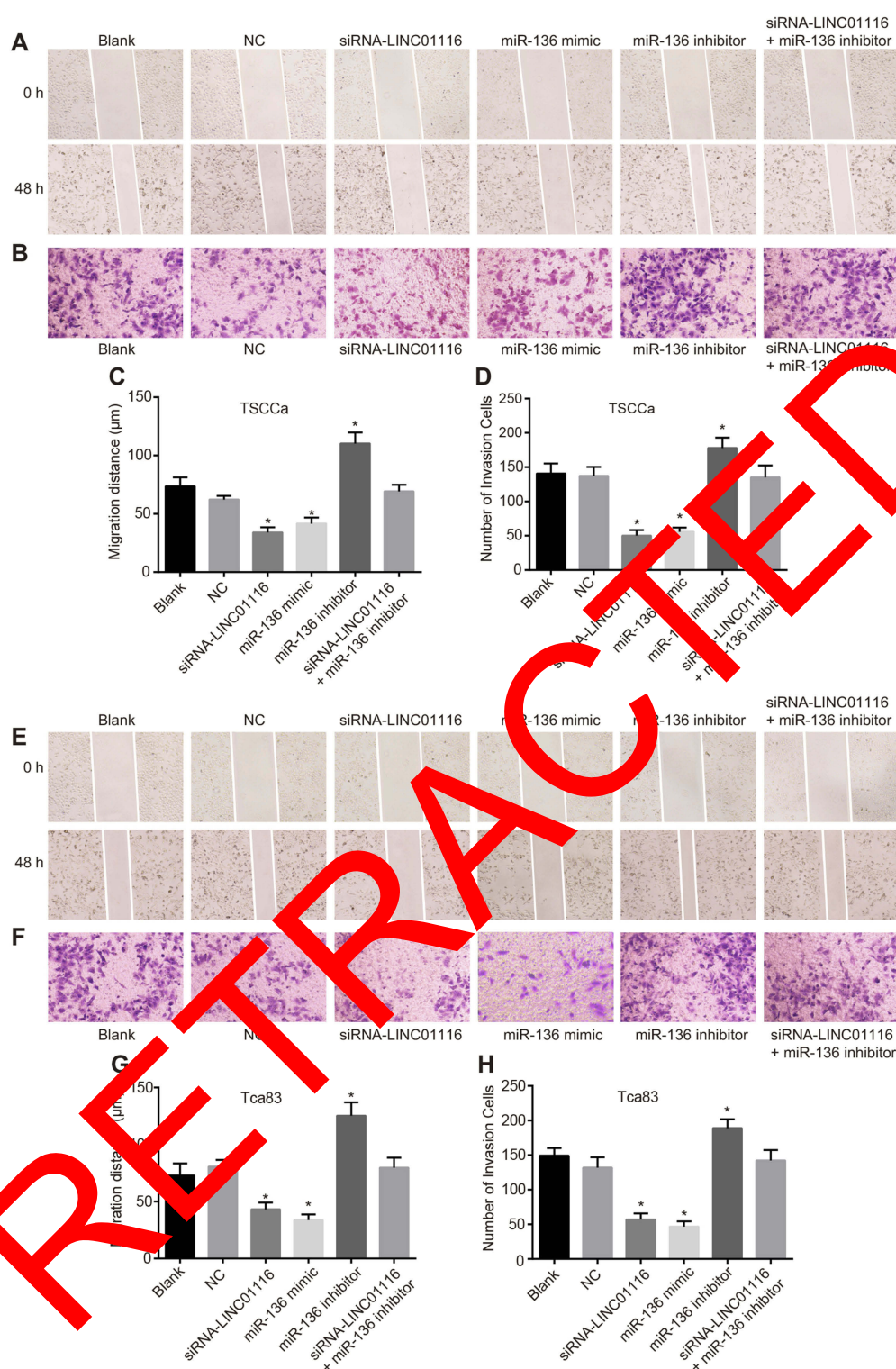
LINC01116 silencing or miR-136 over-expression inhibits tumor growth and LNM in vivo

Tumor xenograft experimentation was performed in nude mice to measure cell tumorigenicity and LNM affected by LINC01116 and miR-136. The results demonstrated (Figure 9) that the tendency of tumor growth and number of LNM in TSCCa cell line and Tca83 cell line was consistent. No obvious changes were present in tumor growth and number of LNM between the blank and NC group (all *p*>0.05). In contrast to the blank and NC groups at the 9th day after inoculation of OSCC cells, the tumor growth rate and the number of LNM were found to be significantly reduced in the miR-136 mimic and siRNA-LINC01116 groups (all *p*<0.05), but elevated in the miR-136 inhibitor group (all *p*<0.05). There were no noticeable differences regarding tumor growth rate or number of LNM in the siRNA-LINC01116 + miR-136 inhibitor

Figure 6 LINC01116 silencing or miR-136 over-expression inhibits the cell viability of OSCC cells. (**A**) Cell viability in TSCCa cell line. (**B**) Cell viability in Tca83 cell line. The data were measurement data and expressed as mean±standard deviation. This experiment was repeated 3 times to obtain the mean value. The repeated measures ANOVA was used to analyze the value comparison at different time points. *p<0.05 vs the blank and NC groups.
**Abbreviations:** miR-136, microRNA-136; OSCC, oral squamous cell carcinoma; CCK-8, Cell Counting Kit-8; ANOVA, analysis of variance; NC, negative control.

Figure 7 LINC01116 silencing or miR-136 over-expression inhibits the cell migration and invasion of OSCC cells. (**A**) Representative images of cell migration in each group of TSCCa cell line. (**B**) Representative images of cell invasion in each group of TSCCa cell line. (**C**) Migration distance in each group of TSCCa cell line. (**D**) The number of invasive cells in each group of TSCCa cell line. (**E**) Representative images of cell migration in each group of Tca83 cell line. (**F**) Representative images of cell invasion in each group of Tca83 cell line. (**G**) Migration distance in each group of Tca83 cell line. (**H**) The number of invasive cells in each group of Tca83 cell line. The data were measurement data and expressed as mean±standard deviation. This experiment was repeated 3 times to obtain the mean value. One-way ANOVA was used for the comparisons among multiple groups. *$p<0.05$ vs the blank and NC groups.
Abbreviations: miR-136, microRNA-136; ANOVA, analysis of variance; NC, negative control.
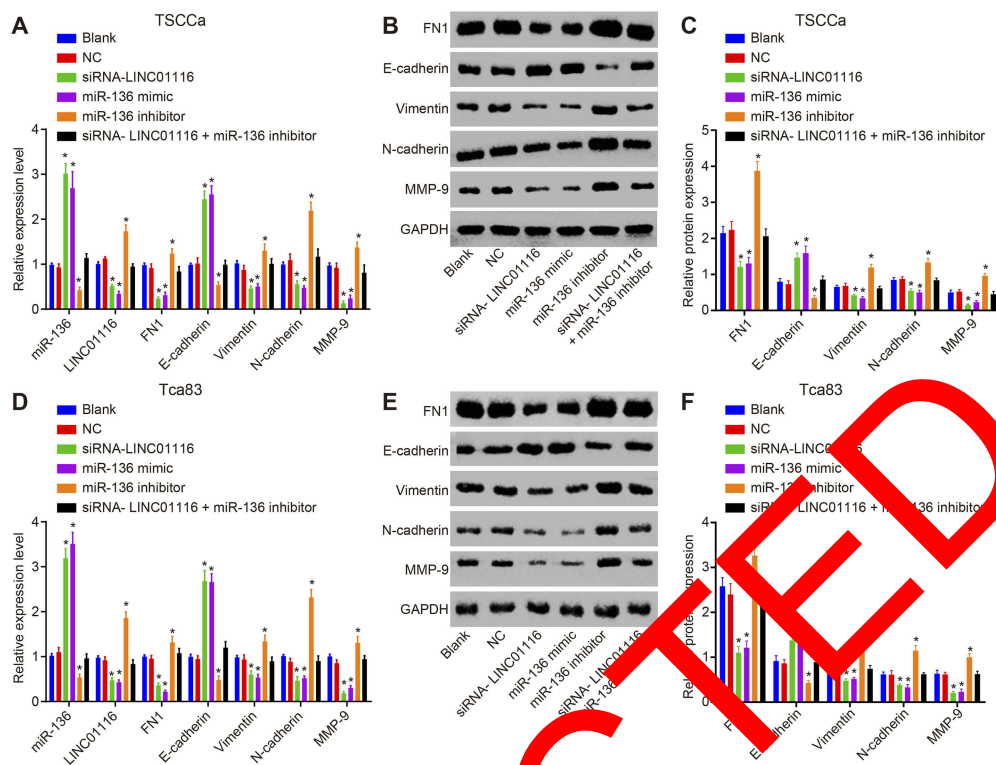
Figure 8 LINC01116 silencing or miR-136 over-expression inhibits the EMT of OSCC cells. (**A**) RT-qPCR was used to determine the relative expression of miR-136, LINC01116, FN1 and EMT-related genes (E-cadherin, Vimentin, N-cadherin, and MMP-9) in each group of TSCCa cell line. (**B, C**) Western blot analysis was used to determine the relative protein expression of FN1 and EMT-related genes (E-cadherin, Vimentin, N-cadherin, and MMP-9) in each group of TSCCa cell line. (**D**) RT-qPCR was used to determine the relative expression of miR-136, LINC01116, FN1 and EMT-related genes (E-cadherin, Vimentin, N-cadherin, and MMP-9) in each group of Tca83 cell line. (**E, F**) Western blot analysis was used to determine the relative protein expression of FN1 and EMT-related genes (E-cadherin, Vimentin, N-cadherin, and MMP-9) in each group of Tca83 cell line. The data were measurement data and expressed as mean±standard deviation. This experiment was repeated 3 times to obtain the mean value. One-way ANOVA was used for comparisons among multiple groups. *$p < 0.05$ vs the blank and NC groups.
Abbreviations: EMT, epithelial–mesenchymal transition; miR-136, microRNA-136; RT-qPCR, reverse transcription quantitative polymerase chain reaction; FN1, fibronectin1; MMP-9, matrix metalloprotein 9; ANOVA, analysis of variance; NC, negative control.

group compared with the blank and NC groups (all $p > 0.05$). Consequently, these findings provided verification attesting that cell tumorigenicity and LNM could be inhibited by down-regulation of LINC01116 or up-regulation of miR-136.

Discussion

OSCC presently remains a major health issue globally and patients typically present with a poor 5-year survival rate.[30] Currently, tissue biopsy and histopathological examination are considered to be the diagnostic means of choice to obtain valuable time to prepare for subsequent treatment of patients plagued by oral cancer.[31] Owing to this reason, the 5-year survival rate of patients diagnosed at early stages exceeds 90%, while leaving 30% of the patients at the late stage to potentially survive.[32] This explains the importance of improvement of early detection techniques and follow-up innovative therapies to improve the quality of life of OSCC patients.[30,33] In addition, LNM

has been identified to be involved in OSCC bringing about undesirable survival rates.[34] Several studies have further demonstrated that the process of EMT is correlated with a decrease in epithelial differentiation and increase in the mesenchymal phenotype, indicating a key step in OSCC progression and metastasis.[35–37] Furthermore, LINC01116 has recently been reported to be involved in multiple carcinomas, such as prostate carcinoma and non-small cell lung carcinoma.[16,17] Additionally, over-expression of FN1 was found in frequent clinical samples obtained from patients with OSCC together with LNM.[34] Based on the literature review and well-designed experiments, the current study tested a hypothesis that LINC01116 potentially plays an important role in the process of OSCC.

Initially, analyses of GEO datasets revealed the abundant expression of LINC01116 and FN1 in OSCC tissues while that of miR-136 was reciprocal, which was successfully verified. In addition, the current experiment demonstrated that LINC01116 could competitively bind to miR-
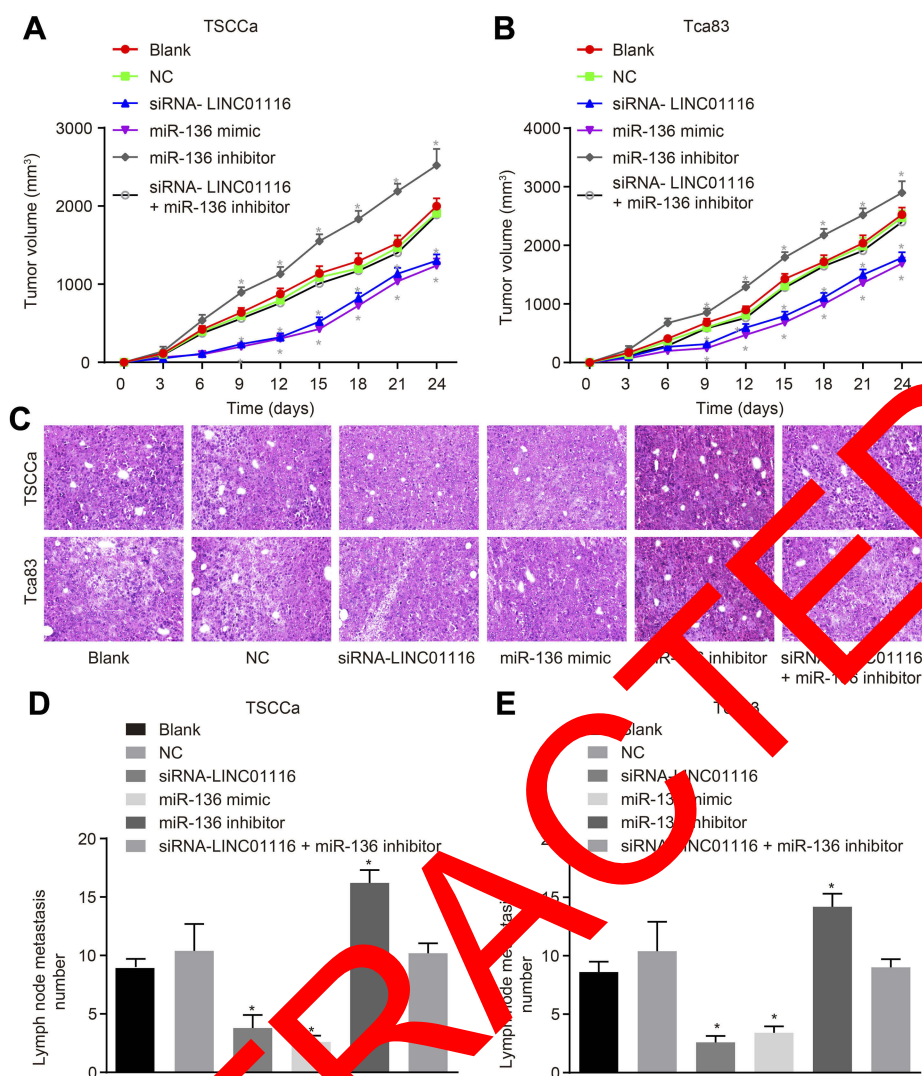
Figure 9 LINC01116 silencing or miR-136 over-expression inhibits the tumor growth and LNM in vivo. (**A**) The tumor growth rate in each group of TSCCa cell line. (**B**) The tumor growth rate in each group of Tca83 cell line. (**C**) HE staining in each group of tumors. (**D**) The number of LNM of TSCCa cell line. (**E**) The number of LNM of Tca83 cell line. The data were measurement data and expressed as mean±standard deviation. This experiment was repeated 3 times to obtain the mean value. The comparisons among multiple groups were performed based on one-way ANOVA and the value comparisons at different time points were performed using repeated measures ANOVA. *$p<0.05$ *vs* the blank and NC groups.

Abbreviations: LNM, lymph node metastasis; miR-136, microRNA-136; HE, hematoxylin-eosin; ANOVA, analysis of variance; NC, negative control.

136 and further regulate the expression of FN1. Consistent with our results, miR-136 was reported to be significantly under-expressed in OSCC when compared to healthy individuals and patients in remission.[38] A study concerning lung adenocarcinoma verified that miR-136 might serve as a tumor-suppressor to EMT as well as prometastatic traits through Smad2 and Smad3, indicating a novel perspective for potential therapeutic approaches.[39] Similar findings were discussed in another study, which concluded that FN1 down-regulation can be a pivotal marker of OSCC progression to predict lymphatic dissemination for patients with OSCC at a relatively early stage,[40] which might assist in explaining the results presented below.

Additionally, the current study elucidated that down-regulation of LINC01116 could augment the expression of miR-136 and E-cadherin, while suppressing that of FN1, Vimentin, N-cadherin, and MMP-9. Subsequently, the changing tendency caused by miR-136 inhibitors was just on the contrary. All the aforementioned factors functioned in tandem to suppress LNM and EMT in OSCC. E-cadherin, N-cadherin, Vimentin, and MMP-9 are widely known as genes related to the process of EMT and play a pivotal role in tumor metastasis, and were thereby implored in the current study.[41] Hereinto, E-cadherin was a calcium-dependent transmembrane glycoprotein in the epithelial tissue and was essential to cell adhesion molecule as well as
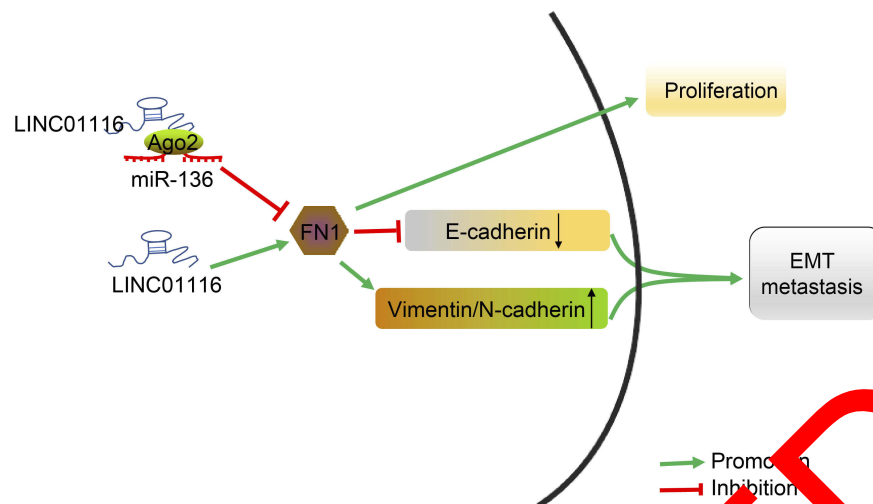
Figure 10 The schematic representation of LINC01116 in the progression of OSCC by regulating miR-136 and FN1. In OSCC cells, the expression of LINC01116 promotes the expression of FN1 through competitively binding to miR-136. Meanwhile, up-regulation of FN1 could promote the proliferation, EMT, and metastasis of OSCC cells, corresponding to inhibited the expression of E-cadherin and promoted the expression of Vimentin, N-cadherin and MMP-9.
Abbreviations: OSCC, oral squamous cell carcinoma; miR-136, microRNA-136; FN1, fibronectin1; MMP-9, matrix metalloprotein-9; E-cadherin, epithelial cadherin; N-cadherin, neural cadherin; EMT, epithelial–mesenchymal transition.

signal transduction in prevention against tumor cell adhesion through the formation of protein complexes attached to the actin cytoskeleton in association with the formation of β-catenin.[42] As a cytoskeletal protein, high expression of Vimentin was found in mesenchymal cells, and several studies have reported that the elevated expression of Vimentin present with a positive relationship with the invasion and metastasis of cancer cells in head and neck squamous cell carcinomas.[43,44] Furthermore, another study suggested the use of N-cadherin as a latent biomarker for timely diagnosis in the early stages of OSCC.[45] Similarly, a previous study mentioned that MMP-9 contributes to the development of proliferation, invasion, and migration in the process of cell and tumor angiogenesis in oral tongue squamous cell carcinoma.[46] Additionally, the expression of E-cadherin and Vimentin was documented to be linked to LNM and tissue location while Vimentin was further related to tumor stage in OSCC in a prior study.[42] Accordingly, we reached the conclusion that LINC01116 silencing or miR-136 over-expression could inhibit EMT and LNM of OSCC tumor in nude mice.

Conclusion

In conclusion, LINC01116 silencing or miR-136 over-expression was demonstrated to inhibit OSCC cell proliferation, migration and invasion, EMT, and LNM via modulation of the LINC01116/miR-136/FN1 axis (Figure 10). Moreover, such regulatory mechanism can be expected to serve as a promising target for the

development of clinical values in OSCC therapy. Additionally, future studies should be more performed with a diverse population, so as to support its promising application in the treatment of OSCC patients.

Acknowledgments

Disclosure

The authors report no conflicts of interest in this work.

References

1. Feng X, Jiang Y, Xie L, et al. Overexpression of proteasomal activator PA28alpha serves as a prognostic factor in oral squamous cell carcinoma. *J Exp Clin Cancer Res*. 2016;35:35. doi:10.1186/s13046-016-0444-6
2. Radhika T, Jeddy N, Nithya S, Muthumeenakshi RM. Salivary biomarkers in oral squamous cell carcinoma - an insight. *J Oral Biol Craniofac Res*. 2016;6(Suppl 1):S51–S54. doi:10.1016/j.jobcr.2016.07.003
3. Chang CC, Yang YJ, Li YJ, et al. MicroRNA-17/20a functions to inhibit cell migration and can be used a prognostic marker in oral squamous cell carcinoma. *Oral Oncol*. 2013;49(9):923–931. doi:10.1016/j.oraloncology.2013.03.430

4. Khangura RK, Sengupta S, Sircar K, Sharma B, Singh S, Rastogi V. HPV involvement in OSCC: correlation of PCR results with light microscopic features. *J Oral Maxillofac Pathol*. 2013;17(2):195–200. doi:10.4103/0973-029X.119756

5. Chaturvedi AK, Anderson WF, Lortet-Tieulent J, et al. Worldwide trends in incidence rates for oral cavity and oropharyngeal cancers. *J Clin Oncol*. 2013;31(36):4550–4559. doi:10.1200/JCO.2013.50.3870

6. Sasahira T, Kurihara M, Bhawal UK, et al. Downregulation of miR-126 induces angiogenesis and lymphangiogenesis by activation of VEGF-A in oral cancer. *Br J Cancer*. 2012;107(4):700–706. doi:10.1038/bjc.2012.330

7. Marsh D, Suchak K, Moutasim KA, et al. Stromal features are predictive of disease mortality in oral cancer patients. *J Pathol*. 2011;223(4):470–481. doi:10.1002/path.2830

8. Sasahira T, Kurihara M, Nishiguchi Y, Fujiwara R, Kirita T, Kuniyasu H. NEDD 4 binding protein 2-like 1 promotes cancer cell invasion in oral squamous cell carcinoma. *Virchows Arch*. 2016;469 (2):163–172. doi:10.1007/s00428-016-1955-4

9. Sasahira T, Kirita T, Kuniyasu H. Update of molecular pathobiology in oral cancer: a review. *Int J Clin Oncol*. 2014;19(3):431–436. doi:10.1007/s10147-014-0684-4

10. Huang WC, Chan SH, Jang TH, et al. miRNA-491-5p and GIT1 serve as modulators and biomarkers for oral squamous cell carcinoma invasion and metastasis. *Cancer Res*. 2014;74(3):751–764. doi:10.1158/0008-5472.CAN-13-1297

11. Wang KC, Chang HY. Molecular mechanisms of long noncoding RNAs. *Mol Cell*. 2011;43(6):904–914. doi:10.1016/j.molcel.2011. 08.018

12. Martens-Uzunova ES, Bottcher R, Croce CM, Jenster G, Visakorpi T, Calin GA. Long noncoding RNA in prostate, bladder, and kidney cancer. *Eur Urol*. 2014;65(6):1140–1151. doi:10.1016/j.eururo.2013. 12.003

13. Zhu M, Chen Q, Liu X, et al. lncRNA H19/miR-675 axis represses prostate cancer metastasis by targeting TGFBI. *Febs J*. 2014;281 (16):3766–3775. doi:10.1111/febs.12902

14. Hua Q, Lv X, Gu X, et al. Genetic variants in lncRNA H19 are associated with the risk of bladder cancer in a Chinese population. *Mutagenesis*. 2016;31(5):531–538. doi:10.1093/mutage/gew018

15. Xiao H, Tang K, Liu P, et al. LncRNA MALAT1 functions as a competing endogenous RNA to regulate ZEB2 expression by sponging miR-200s in clear cell kidney carcinoma. *Oncotarget*. 2015;6(35):38005–38015. doi:10.18632/oncotarget.5357

16. Beaver LM, Kuintzle R, Buchanan A, et al. Long noncoding RNAs and sulforaphane: a target for chemoprevention and suppression of prostate cancer. *J Nutr Biochem*. 2017;42:72–83. doi:10.1016/j. jnutbio.2017.01.001

17. Liang Y, Ma Y, Li J, et al. Effect of long non-coding RNA LINC01116 on biological behaviors of non-small cell lung cancer cells via the hippo signaling pathway [Retraction]. *J Cell Biochem*. 2018. doi:10.1002/jcb.26711

18. Bartonicek N, Maag JL, Dinger ME. Long noncoding RNAs in cancer: mechanisms of action and technological advancements. *Mol Cancer*. 2016;15:43. doi:10.1186/s12943-016-0530-6

19. Schmitt AM, Chang HY. Long noncoding RNAs in cancer pathways. *Cancer Cell*. 2016;29(4):452–463. doi:10.1016/j. ccell.2016.03.010

20. Gao W, Liu Y, Qin R, Liu D, Feng Q. Silence of fibronectin 1 increases cisplatin sensitivity of non-small cell lung cancer cell line. *Biochem Biophys Res Commun*. 2016;476(1):35–41. doi:10.1016/j. bbrc.2016.05.081

21. Yen CY, Huang CY, Hou MF, et al. Evaluating the performance of fibronectin 1 (FN1), integrin alpha4beta1 (ITGA4), syndecan-2 (SDC2), and glycoprotein CD44 as the potential biomarkers of oral squamous cell carcinoma (OSCC). *Biomarkers*. 2013;18(1):63–72. doi:10.3109/1354750X.2012.737025

22. Kong D, Zhang G, Ma H, Jiang G. miR-1271 inhibits OSCC cell growth and metastasis by targeting ALK. *Neoplasma*. 2015;62 (4):559–566. doi:10.4149/neo_2015_067

23. Liu C, Wang Z, Wang Y, Gu W. MiR-338 suppresses the growth and metastasis of OSCC cells by targeting NRP1. *Mol Cell Biochem*. 2015;398(1–2):115–122. doi:10.1007/s11010-014-2211-3

24. Zhao H, Liu S, Wang G, et al. Expression of miR-136 is associated with the primary cisplatin resistance of human epithelial ovarian cancer. *Oncol Rep*. 2015;33(2):591–598. doi:10.3892/ or.2014.3640

25. Shen S, Yue H, Li Y, et al. Upregulation of miR-136 in human non-small cell lung cancer cells promotes Erk1/2 activation by targeting PPP2R2A. *Tumour Biol*. 2014;35(1):631–640. doi:10.1007/ s13277-013-1087-2

26. Fujita A, Sato JR, Rodrigues Lde O, Ferreira CE, Sogayar MC. Evaluating different methods of microarray data normalization. *BMC Bioinformatics*. 2006;7:469. doi:10.1186/1471-2105-7-469

27. Smyth GK. Linear models and empirical bayes methods for assessing differential expression in microarray experiments. *Stat Appl Genet Mol Biol*. 2004;3:Article3. doi:10.2202/1544-6115.1027

28. Ratnapradipa KL, Lian M, Jeffe DB, et al. Patient, hospital, and geographic disparities in laparoscopic surgery use among surveillance, epidemiology, and end results-medicare patients with colon cancer. *Dis Colon Rectum*. 2017;60(9):905–913. doi:10.1097/ DCR.0000000000000874

29. Tuo YL, Li XM, Luo J. Long noncoding RNA UCA1 modulates breast cancer cell growth and apoptosis through decreasing tumor suppressive miR-143. *Eur Rev Med Pharmacol Sci*. 2015;19 (18):3403–3411.

30. Rao SK, Pavicevic Z, Du Z, et al. Pro-inflammatory genes as biomarkers and therapeutic targets in oral squamous cell carcinoma. *J Biol Chem*. 2010;285(42):32512–32521. doi:10.1074/jbc. M110.150490

31. Carreras-Torras C, Gay-Escoda C. Techniques for early diagnosis of oral squamous cell carcinoma: systematic review. *Med Oral Patol Oral Cir Bucal*. 2015;20(3):e305–e315. doi:10.4317/ medoral.20347

32. Omar E. Future imaging alternatives: the clinical non-invasive modalities in diagnosis of oral squamous cell carcinoma (OSCC). *Open Dent J*. 2015;9:311–318. doi:10.2174/1874210601509010311

33. Brocklehurst PR, Baker SR, Speight PM. A qualitative study examining the experience of primary care dentists in the detection and management of potentially malignant lesions. 1. Factors influencing detection and the decision to refer. *Br Dent J*. 2010;208(2):E3; discussion 72–73. doi:10.1038/sj.bdj.2010.54

34. Morita Y, Hata K, Nakanishi M, et al. Cellular fibronectin 1 promotes VEGF-C expression, lymphangiogenesis and lymph node metastasis associated with human oral squamous cell carcinoma. *Clin Exp Metastasis*. 2015;32(7):739–753. doi:10.1007/s10585-015-9741-2

35. Iwata E, Hasegawa T, Takeda D, et al. Transcutaneous carbon dioxide suppresses epithelial-mesenchymal transition in oral squamous cell carcinoma. *Int J Oncol*. 2016;48(4):1493–1498. doi:10.3892/ ijo.2016.3380

36. Smith A, Teknos TN, Pan Q. Epithelial to mesenchymal transition in head and neck squamous cell carcinoma. *Oral Oncol*. 2013;49 (4):287–292. doi:10.1016/j.oraloncology.2012.10.009

37. Zhang S, Zhou X, Wang B, et al. Loss of VHL expression contributes to epithelial-mesenchymal transition in oral squamous cell carcinoma. *Oral Oncol*. 2014;50(9):809–817. doi:10.1016/j. oraloncology.2014.06.007

38. Momen-Heravi F, Trachtenberg AJ, Kuo WP, Cheng YS. Genomewide study of salivary microRNAs for detection of oral cancer. *J Dent Res*. 2014;93(7 Suppl):86S–93S. doi:10.1177/ 0022034514531018

39. Yang Y, Liu L, Cai J, et al. Targeting Smad2 and Smad3 by miR-136 suppresses metastasis-associated traits of lung adenocarcinoma cells. *Oncol Res*. 2013;21(6):345–352. doi:10.3727/096504014X14024160459285

40. Zhang Z, Pan J, Li L, Wang Z, Xiao W, Li N. Survey of risk factors contributed to lymphatic metastasis in patients with oral tongue cancer by immunohistochemistry. *J Oral Pathol Med*. 2011;40(2):127–134. doi:10.1111/j.1600-0714.2010.00953.x

41. Li W, Ma J, Ma Q, et al. Resveratrol inhibits the epithelial-mesenchymal transition of pancreatic cancer cells via suppression of the PI-3K/Akt/NF-kappaB pathway. *Curr Med Chem*. 2013;20(33):4185–4194.

42. Zhou J, Tao D, Xu Q, Gao Z, Tang D. Expression of E-cadherin and vimentin in oral squamous cell carcinoma. *Int J Clin Exp Pathol*. 2015;8(3):3150–3154.

43. Nijkamp MM, Span PN, Hoogsteen IJ, van der Kogel AJ, Kaanders JH, Bussink J. Expression of E-cadherin and vimentin correlates with metastasis formation in head and neck squamous cell carcinoma patients. *Radiother Oncol*. 2011;99(3):344–348. doi:10.1016/j.radonc.2011.05.066

44. Liu S, Liu L, Ye W, et al. High vimentin expression associated with lymph node metastasis and predicated a poor prognosis in oral squamous cell carcinoma. *Sci Rep*. 2016;6:38834. doi:10.1038/srep38834

45. Chandolia B, Rajliwal JP, Bajpai M, Arora M. Prognostic potential of N-cadherin in oral squamous cell carcinoma via immunohistochemical methods. *J Coll Physicians Surg Pak*. 2017;27(8):475–478.

46. Fan HX, Wang S, Zhao H, et al. Sonic hedgehog signaling may promote invasion and metastasis of oral squamous cell carcinoma by activating MMP-9 and E-cadherin expression. *Med Oncol*. 2014;31(7):41. doi:10.1007/s12032-014-0074-0